

# Transverse magneto-optical Kerr effect measured using phase modulation

**K. Postava**

kamil.postava@vsb.cz

Laboratory of Magnetism, Institute of Experimental Physics, University of Bialystok, 41 Lipowa Street, 15-424 Bialystok, Poland

Department of Physics, Technical University Ostrava, 17. listopadu 15, 708 33 Ostrava-Poruba, Czech Republic

Research Institute of Electronics, Shizuoka University, Johoku 3-5-1, Hamamatsu 432-8011, Japan

**A. Maziewski**

Laboratory of Magnetism, Institute of Experimental Physics, University of Bialystok, 41 Lipowa Street, 15-424 Bialystok, Poland

**A. Stupakiewicz**

Laboratory of Magnetism, Institute of Experimental Physics, University of Bialystok, 41 Lipowa Street, 15-424 Bialystok, Poland

**A. Wawro**

Institute of Physics, Polish Academy of Sciences, Al. Lotnikow 32/46, 02-668 Warsaw, Poland

**L. T. Baczewski**

Institute of Physics, Polish Academy of Sciences, Al. Lotnikow 32/46, 02-668 Warsaw, Poland

**Š. Višňovský**

Institute of Physics, Charles University, Ke Karlovu 5, 121 16 Prague 2, Czech Republic

**T. Yamaguchi**

Research Institute of Electronics, Shizuoka University, Johoku 3-5-1, Hamamatsu 432-8011, Japan

An ellipsometric configuration for measurement of the complex transverse magneto-optical Kerr effect is described that uses a photoelastic modulator (PEM). The real and imaginary parts of the complex transverse Kerr effect are represented as small perturbations of ellipsometric angles  $\psi$  and  $\Delta$ . The measurement, based on null ellipsometry and zone averaging, gives high signal typical for modulation techniques and insensitivity to other magnetisation components and system imperfections. The method is demonstrated by the measurement of transverse component during magnetisation reversal in a thin cobalt film. [DOI: 10.2971/jeos.2006.06017]

**Keywords:** Transverse magneto-optic Kerr effect, phase modulation, null ellipsometry, photoelastic modulator

## 1 Introduction

Magneto-optical (MO) methods have been established as commonly used nondestructive techniques for study of thin-film and surface magnetism. Particularly magneto-optic vector magnetometry is widely used for monitoring of magnetisation reversal and magnetic anisotropy. Three components of the magnetisation vector are usually distinguished: the polar component  $M_P$  (perpendicular to film interfaces), the longitudinal  $M_L$  (in-plane component parallel to the plane of light incidence), and the transverse magnetisation component  $M_T$  (perpendicular to the plane of incidence) [1]–[5]. Modulation techniques with photoelastic modulator (PEM) [6, 7], which propose strong signals, are often used for rotation and ellipticity measurements originating from the polar and longitudinal Kerr effects. Various techniques have been used for separation of the polar and longitudinal contribution in the frame of MO vector magnetometry [8]–[12].

On the other hand, the transverse Kerr effect can be measured as a change in reflectivity of  $p$ -polarised light [13]–[17] and is mainly applied for in-plane magnetisation monitoring. The microscopic origin of the transverse Kerr effect and available information about a material are similar to that of the longi-

tudinal Kerr effect. However, at transverse magnetization the optical access even for angles of incidence close to the grazing incidence can be accomplished with minimum restrictions on the shape of electromagnet pole pieces. In this way, higher in-plane magnetic fields can be applied to the sample. Moreover, the method of rotation of the magnetic field and a sample [2] to separate magnetisation components is problematic for some special and *in-situ* measurements. In such cases, two in-plane magnetisation components can be measured by the longitudinal and transverse MO effects and separated only by change of optical configuration.

Phase modulation techniques with a PEM were applied for transverse Kerr effect measurement by several authors [10, 18, 19]. Jordan and Whiting [18] modified the method with variable azimuth of the polariser [3] measuring a combination of longitudinal and transverse MO effect. Unfortunately, the separation of the two in-plane magnetisation components remains difficult. An interesting technique of transverse Kerr effect measurement using a PEM was presented by Osgood [19] and Vavassori [10]. The authors use a Polarizer-Sample-PEM-Analyzer system to detect the real part of the transverse

Kerr effect using signal at the second harmonic frequency of the modulator. However, the configuration does not allow the measurement of the complex transverse Kerr effect.

In this paper, we propose a new configuration for transverse Kerr effect measurement based on a null ellipsometry with phase modulation. First, the complex transverse Kerr effect is defined as a small perturbation of the standard ellipsometric angles  $\psi$  and  $\Delta$ . Then we propose transverse MO effect measurement using a Polariser-PEM-Sample-Compensator-Analyser (PMSCA) system based on nulling ellipsometry described in Ref. [20]. In the last part of this paper, the technique is experimentally demonstrated on transverse hysteresis loop measurements of a thin cobalt film.

## 2 COMPLEX TRANSVERSE KERR EFFECT

The optical and linear magneto-optical response of the sample can be described using the Jones reflection matrix

$$\mathbf{R} = \begin{pmatrix} r_{ss} & r_{ps}(M_T, M_L) \\ r_{sp}(M_T, M_L) & r_{pp}(M_T) \end{pmatrix} \quad (1)$$

consisting of the amplitude reflection coefficients. The polar and longitudinal MO effects are observed using the conversion reflection coefficients  $r_{sp}$  and  $r_{ps}$ , which relates to the Kerr rotation  $\theta$  and ellipticity  $\epsilon$  for  $s$ - and  $p$ -polarised incident beam by the relations  $\theta_s + i\epsilon_s = r_{sp}/r_{ss}$  and  $\theta_p + i\epsilon_p = -r_{ps}/r_{pp}$ , respectively. However, the transverse Kerr effect can be expressed as a change of the coefficient  $r_{pp}(\mathbf{M}) = r_{pp}(0) + \Delta r_{pp}(M_T)$ . Figure 1 shows typical configuration, which uses differential reflectivity of  $p$ -polarised light.

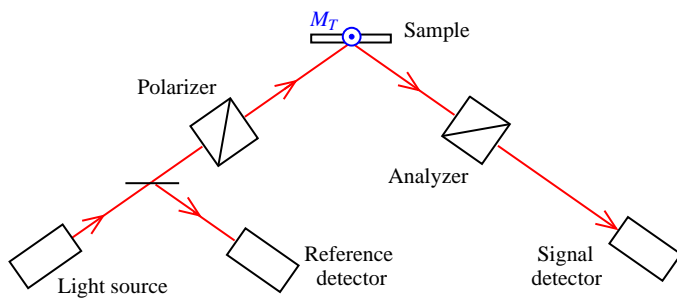


FIG. 1 Standard differential intensity configuration for transverse Kerr effect ( $M_T$  is perpendicular to the plane of incidence). Polariser and analyser are adjusted to  $p$ -direction (parallel to the plane of incidence). Difference between intensities at the signal and reference detectors is proportional to  $M_T$ .

Note that in this configuration PEM can be used only for modulation of light intensity [21]. The relative difference between intensities measured with signal and reference detectors can be expressed in the form

$$\frac{\Delta I}{I_0} = \frac{|r_{pp}(M_T)|^2 - |r_{pp}(0)|^2}{|r_{pp}(0)|^2} \approx 2 \Re \left\{ \frac{\Delta r_{pp}(M_T)}{r_{pp}(0)} \right\}, \quad (2)$$

where we have made use the relation  $|r_{pp}|^2 = r_{pp} r_{pp}^*$ . The second order term  $|\Delta r_{pp}(M_T)/r_{pp}(0)|^2$  is neglected. The reflection coefficients are generally complex quantities. Figure 2

shows an example of the modelled angular dependence of the complex transverse Kerr effect for cobalt thin film.

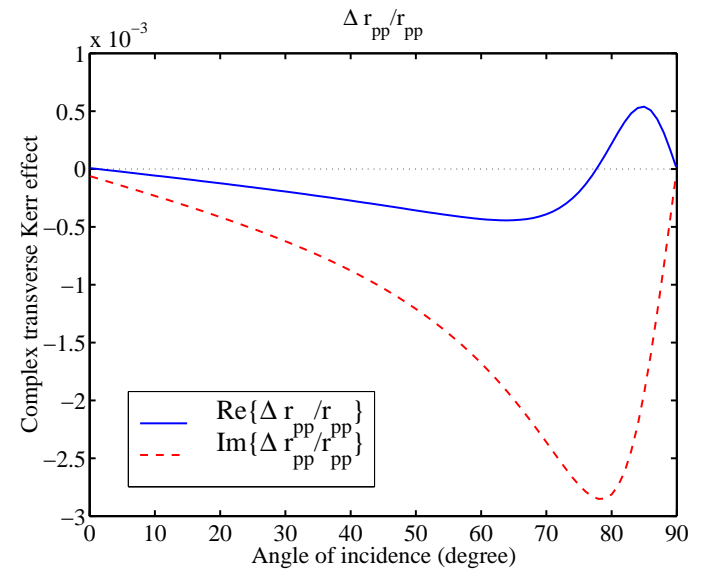


FIG. 2 Example of the modelled complex transverse MO Kerr effect for the structure  $\text{Al}_2\text{O}_3/\text{Mo}(20 \text{ nm})/\text{Co}(10 \text{ nm})/\text{Au}(8 \text{ nm})$  and the wavelength of 640 nm.

Optical and magneto-optical constants were taken from Refs. [22, 23]. Not only the real but also the imaginary part of the complex transverse Kerr effect carries valuable information in MO ellipsometry: (i) in some cases, the signal measured by the imaginary part can be stronger (see Figure 2); (ii) measurements of two independent quantities enables to evaluate the complex MO parameters, leading to the complex permittivity tensor components of a material; (iii) the real and imaginary part of the complex transverse MO effect have different sensitivity to linear and quadratic transverse Kerr effects, which can be used for separation of the effects; and (iv) in general, two independent quantities display different depth sensitivities, which may be exploited in the determination of the in-depth profile of the sample.

The real and imaginary part of the complex transverse Kerr effect can be represented as small perturbations to the ellipsometric angles  $\psi = \psi_0 + \delta\psi$  and  $\Delta = \Delta_0 + \delta\Delta$  where  $\tan \psi \exp(i\Delta) = r_{pp}/r_{ss}$ . Assuming  $\delta\psi \ll \psi_0$  and  $\delta\Delta \ll \Delta_0$ , the approximate formulae become

$$\exp[i(\Delta + \delta\Delta)] \approx (1 + i\delta\Delta) \exp(i\Delta), \quad (3)$$

$$\tan(\psi + \delta\psi) \approx \tan \psi + (1 + \tan^2 \psi) \delta\psi. \quad (4)$$

The transverse effect is obtained in the form:

$$\frac{\Delta r_{pp}(M_T)}{r_{pp}(0)} = \frac{2}{\sin 2\psi_0} \delta\psi + i \delta\Delta. \quad (5)$$

Equation (5) shows that the real  $\Re[\Delta r_{pp}(M_T)/r_{pp}(0)]$  and the imaginary part  $\Im[\Delta r_{pp}(M_T)/r_{pp}(0)]$  of the complex transverse MO effect are immediately related to the small changes of the ellipsometric angles  $\psi$  and  $\Delta$ , respectively.

### 3 NEW CONFIGURATION WITH PEM

Figure 3 schematically shows basic components of the proposed null PMSCA (Polariser–Modulator–Sample–Compensator–Analyser) ellipsometric system.

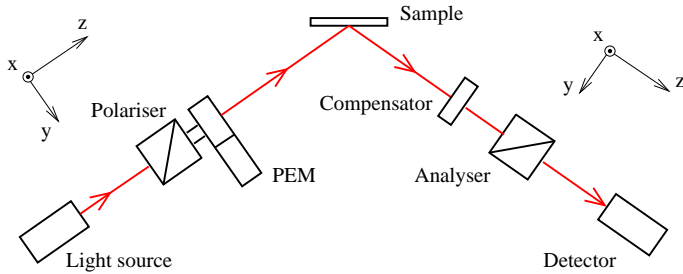


FIG. 3 Proposed null ellipsometry system for transverse Kerr effect measurement.

The system consists of the polariser, which is mechanically connected to the modulator (PEM) and rotated by the constant angle  $45^\circ$  from the modulator axis. Both components can together slowly rotate (in this paper,  $P$  denotes the azimuth of the modulator stress/strain axis). The polarisation state of reflected light from the sample is measured with a quarter-wave compensator (retardation angle  $\phi = 90^\circ$  and azimuth  $C = \pm 45^\circ$ ) and an analyser with the adjustable azimuth angle  $A$ . The retardation angle of PEM is a time-harmonic function

$$\varphi = \varphi_A \sin \omega t, \quad (6)$$

where  $\omega = 2\pi f$  is the angular frequency of the PEM phase oscillation and  $\varphi_A$  denotes the modulation amplitude. The intensity at the detector can be expressed as

$$I = I_0 + I_S \sin \varphi + I_C \cos \varphi. \quad (7)$$

In terms of the Bessel functions of first kind  $J_n$ , the terms  $\sin \varphi$  and  $\cos \varphi$  can be expanded using Eq. (6) into the series  $\sin \varphi = 2J_1(\varphi_A) \sin \omega t + \dots$  and  $\cos \varphi = J_0(\varphi_A) + 2J_2(\varphi_A) \cos 2\omega t + \dots$ . Consequently, Eq. (7) can be rewritten in the form:

$$I = I'_0 + I_\omega \sin \omega t + I_{2\omega} \cos 2\omega t, \quad (8)$$

where  $I'_0 = I_0 + J_0(\varphi_A) I_C$ ,  $I_\omega = 2J_1(\varphi_A) I_S$ , and  $I_{2\omega} = 2J_2(\varphi_A) I_C$ . For an easy calibration, we propose to adjust the modulation amplitude  $\varphi_A = 137.79^\circ$  for which  $J_0 = 0$ ,  $J_1 = 0.51915$ , and  $J_2 = 0.43175$ .

The complex transverse Kerr effect measurement is performed in two steps. In the first step, the azimuths of Polariser-PEM system and Analyser are adjusted to obtain null signal at the first and second harmonic frequency simultaneously (the details on the nulling procedure can be found in Ref. [20]). There are eight different sets of azimuths  $P$  and  $A$  (called the null zones), for which the null signal is obtained. In the second step, the real  $\Re(\Delta r_{pp}/r_{pp})$  and the imaginary part  $\Im(\Delta r_{pp}/r_{pp})$  of the complex transverse Kerr effect is proportional to change of the second  $I_{2\omega}$  and first harmonic signal  $I_\omega$ , respectively.

An important aspect of this technique is its insensitivity to the polar  $M_P$  and longitudinal  $M_L$  magnetisation components. These are eliminated by averaging the signal from two different zones. Using Jones matrix calculus the signals measured at first and second harmonic frequency are obtained in the form:

$$\frac{I_S}{I_0} = (\pm)_C (\pm)_A \sin 2\psi_0 \Im \left\{ \frac{\Delta r_{pp}}{r_{pp}} \right\} + \sin 2\psi_0 [(\theta_s - \theta_p) \sin \Delta_0 - (\epsilon_s + \epsilon_p) \cos \Delta_0] \quad (9)$$

$$\frac{I_C}{I_0} = (\pm)_C (\pm)_P (\pm)_A \sin 2\psi_0 \Re \left\{ \frac{\Delta r_{pp}}{r_{pp}} \right\} + (\mp)_P \sin 2\psi_0 [(\theta_s + \theta_p) \cos \Delta_0 + (\epsilon_s - \epsilon_p) \sin \Delta_0] \quad (10)$$

The signs  $(\pm)_C$  correspond to different azimuths of compensator  $C = \pm 45^\circ$ . Similarly,  $(\pm)_A$  and  $(\pm)_P$  describe nulls in different zones of Analyser and Polariser-PEM system. From Eqs. (9) and (10) it is clear that the polar and longitudinal Kerr rotations  $\theta_{s,p}$  and ellipticities  $\epsilon_{s,p}$  can be easily subtracted from the transverse Kerr effect using averaging of signals from two zones obtained for different compensator or analyser azimuths. An important aspect of the method is its insensitivity to azimuth errors of polariser-PEM system, analyser, which, after zone averaging, eliminates the azimuth error of the compensator. In quantitative measurements the system can be calibrated using a standard way [6] and the ellipsometric angle  $\psi_0$  is obtained from the azimuth of Polariser-PEM system [20]. We note that the polarising components in the incident and reflected arms can be exchanged. Therefore, the Polariser-Compensator-Sample-Modulator-Analyser (PC-SMA) system can be similarly used if more appropriate in a specific user's application.

### 4 EXPERIMENTAL DEMONSTRATION

The technique is demonstrated on transverse hysteresis loops taken with in-plane magnetic field in the structure  $\text{Al}_2\text{O}_3/\text{Mo}(20 \text{ nm})/\text{Co}(10 \text{ nm})/\text{Au}(8 \text{ nm})$ . The Co film epitaxially grown on Mo(110) buffer shows strong uniaxial magnetic anisotropy originating from lattice mismatch between Co and Mo. A detailed description of the sample's magnetic properties was reported in Ref [24]. The magnetic field was applied close to the hard (magnetic) axis which results in coherent rotation of magnetisation during reversal (magnetization) process. Figure 4 shows the technique of averaging of the hysteresis loops obtained in different zones for  $C = \pm 45^\circ$  to obtain the complex transverse Kerr signal. The angle of incidence of  $45^\circ$  and the laser beam of wavelength of 640 nm were used. Figure 4 demonstrates the elimination by zone averaging of the longitudinal Kerr effect.

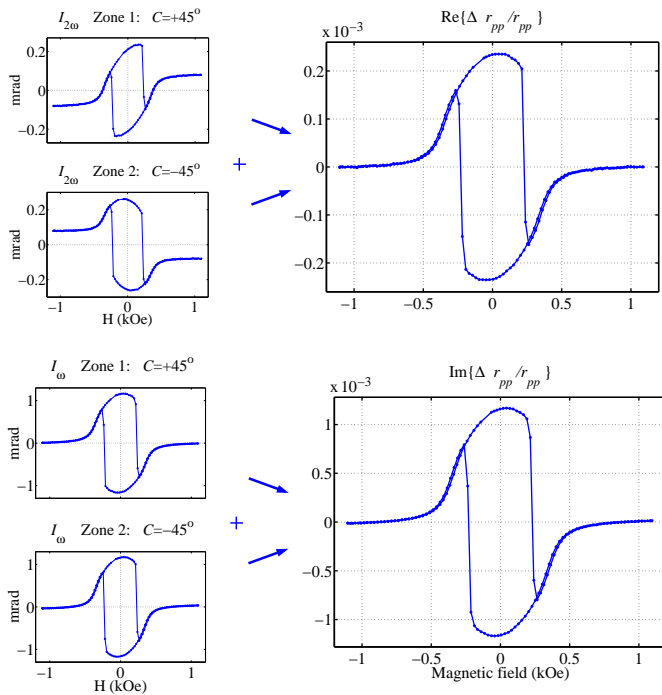


FIG. 4 Measurement of the complex transverse Kerr effect using the proposed method is demonstrated on the structure  $\text{Al}_2\text{O}_3/\text{Mo}(20\text{ nm})/\text{Co}(10\text{ nm})/\text{Au}(8\text{ nm})$ . Upper and lower subplot correspond to measurement of  $\Re\{\Delta r_{pp}/r_{pp}\}$  and  $\Im\{\Delta r_{pp}/r_{pp}\}$ , respectively. Averaging in different zones obtained for  $C = \pm 45^\circ$  eliminates the longitudinal contribution. Obtained loops show mainly coherent rotation of the magnetisation. For high field the magnetisation vector is forced into the field direction and the measured transverse component vanish. However, in remanent state (for zero field) the magnetisation rotates to the easy axis and the transverse Kerr effect is maximal.

In the present case, a more important manifestation of the longitudinal Kerr effect is observed in  $\Re(\Delta r_{pp}/r_{pp})$  than in  $\Im(\Delta r_{pp}/r_{pp})$ . Clearly, the shapes of the averaged loops measured as a field dependence of  $\Re(\Delta r_{pp}/r_{pp})$  and  $\Im(\Delta r_{pp}/r_{pp})$  are the same. We note that the quadratic transverse effect (proportional to  $M_T^2$ ) was eliminated from the measurement.

## 5 CONCLUSION

In conclusion, we summarise the advantages of the proposed technique: (i) a complete information on the transverse Kerr effect in terms of the complex quantities  $\Re\{\Delta r_{pp}/r_{pp}\}$  and  $\Im\{\Delta r_{pp}/r_{pp}\}$  can be obtained, (ii) due to the phase modulation, the signal is reasonably strong with a high signal-to-noise ratio, (iii) the zone averaging enables elimination of the longitudinal and polar Kerr effect contributions, and (iv) the proposed method is insensitive to the initial azimuth error of the analyser, compensator, and polariser-PEM system. The technique can be applied in both the MO vector magnetometer and MO spectroscopy.

## ACKNOWLEDGEMENTS

This work has been done in the frame of the Marie Curie Host Fellowships for Transfer of Knowledge – the NANOMAG-LAB project (2004-003177). Partial support from the project KAN 400100653, MSM6198910016, and from the

Grant Agency of the Czech Republic (202/06/0531) is acknowledged.

## References

- [1] Z. J. Yang and M. R. Scheinfein, "Combined three-axis surface magneto-optical Kerr effects in the study of surface and ultrathin-film magnetism" *J. Appl. Phys.* **74**, 6810–6823 (1993).
- [2] C. Daboo, J. A. C. Bland, R. J. Hicken, A. J. R. Ives, M. J. Baird, and M. J. Walker, "Vectorial magnetometry with the magneto-optic Kerr effect applied to Co/Cu/Co trilayer structures" *Phys. Rev. B* **47**, 11852–11859 (1993).
- [3] J. M. Florczak and E. Dan Dahlberg, "Detecting two magnetization components by the magneto-optical Kerr effect" *J. Appl. Phys.* **67**, 7520–7525 (1990).
- [4] H. Ohldag, N. B. Weber, F. U. Hillebrecht, and E. Kisker, "Observation of in plane magnetization reversal using polarization dependent magneto-optic Kerr effect" *J. Appl. Phys.* **91**, 2228–2231 (2002).
- [5] Š. Višňovský, R. Lopušník, M. Bauer, J. Bok, J. Rassbender, and B. Hillebrands, "Magneto-optic ellipsometry in multilayers at arbitrary magnetization" *Opt. Express* **9**, 121–135 (2001).
- [6] K. Sato, "Measurement of magneto-optical Kerr effect using piezobirefringent modulator" *Jap. J. Appl. Phys.* **20**, 2403–2409 (1981).
- [7] J. Badoz, M. Billardon, J. Canit, and M. F. Russel, "Sensitive devices to determine the state and degree of polarization of a light beam using a birefringence modulator" *J. Optics (Paris)* **8**, 373–384 (1977).
- [8] H. F. Ding, S. Pütter, H. Oepen, and J. Kirschner, "Experimental method for separating longitudinal and polar Kerr signals" *J. Magn. Magn. Mater.* **212**, 5–11 (2000).
- [9] H. F. Ding, S. Pütter, H. P. Oepen, and J. Kirschner, "Spin-reorientation transition in thin films studied by the component-resolved Kerr effect" *Phys. Rev. B* **63**, 134425–1–134425–7 (2001).
- [10] P. Vavassori, "Polarization modulation technique for magneto-optical quantitative vector magnetometry" *Appl. Phys. Lett.* **77**, 1605–1607 (2000).
- [11] S.-C. Shin, J.-W. Lee, S.-K. Kim, and J. Kim, "In situ vectorial magnetization reversal study of ultrathin Co films on Pd (111) using magneto-optical Kerr effects" *Appl. Phys. Lett.* **81**, 91–93 (2002).
- [12] J.-W. Lee, J. Kim, S.-K. Kim, J.-R. Jeong, and S.-C. Shin, "Full vectorial spin-reorientation transition and magnetization reversal study in ultrathin ferromagnetic films using magneto-optical Kerr effects" *Phys. Rev. B* **65**, 144437–1–144437–7 (2002).
- [13] A. K. Zvezdin and V. A. Kotov, *Modern Magneto-optics and Magneto-optical materials* (Institute of Physics Publishing, Bristol and Philadelphia, 1997).
- [14] Š. Višňovský, *Optics in magnetic multilayers and nanostructures* (CRC Press, Taylor & Francis, 2006).
- [15] C. Penfold, R. T. Collins, A. P. B. Tufaile, and Y. Souche, "Transverse magneto-optical Kerr effect: the phase change of reflected light" *J. Magn. Magn. Mater.* **242–245**, 964–966 (2002).
- [16] Y. Souche, A. P. B. Tufaile, C. E. Santi, V. Novosad, and A. D. Santos, "Figure of merit for transverse magneto-optical Kerr effect" *J. Magn. Magn. Mater.* **226–230**, 1686–1687 (2001).
- [17] K. Postava, J. Pištora, and Š. Višňovský, "Magneto-optical effects in ultrathin structures at transversal magnetization" *Czech J. Phys. B* **49**, 1185–1204 (1999).

- [18] S. M. Jordan and J. S. S. Whiting, "Detecting two components of magnetization in magnetic layer structures by use of a photoelastic modulator" *Rev. Sci. Instrum.* **67**, 4286–4289 (1996).
- [19] R. M. Osgood III, S. D. Bader, B. M. Clemens, R. L. White, and H. Matsuyama, "Second-order magneto-optic effects in anisotropic thin films" *J. Magn. Magn. Mater.* **182**, 297–323 (1998).
- [20] K. Postava, A. Maziewski, T. Yamaguchi, R. Ossikovski, Š. Višňovský, and J. Pištorá, "Null ellipsometer with phase modulation" *Opt. Express* **12**, 6040–6045 (2004).
- [21] T. C. Oakberg, "Magneto-optic Kerr effect", HINDS Instruments (2005).
- [22] P. B. Johnson and R. W. Christy, "Optical constants of transition metals: Ti, V, Cr, Mn, Fe, Co, Ni, and Pd" *Phys. Rev. B* **9**, 5056–5070 (1974).
- [23] Š. Višňovský, M. Nývlt, V. Pařízek, P. Kielar, V. Prosser, and R. Krishnan, "Magneto-optical studies of Pt/Co multilayers and Pt-Co alloy thin films" *IEEE Trans. Magn.* **29**, 3390–3392 (1993).
- [24] A. Stupakiewicz, Z. Kurant, A. Maziewski, L. T. Baczewski, A. Maneikis, and A. Wawro, "Magnetic anisotropy modification in ultrathin Co(0001) film epitaxially grown on Mo(110)" *J. Magn. Magn. Mater.* **290-291**, 242–245 (2005).